Prepared for the
14th International Workshop on Deep Inelastic Scattering, DIS2006, April 20-24, 2006, Tsukuba, Japan
www-h1.desy.de/publications/H1preliminary.short_list.html
H1prelim-06-031

Inclusive Prompt Photon Production in Deep Inelastic Scattering at HERA

H1 Collaboration

Abstract

Results are presented on the inclusive production of isolated prompt photons in deep inelastic scattering with a four-momentum transfer of $Q^2 > 4$ GeV^2. The cross sections are measured for the transverse momentum range of the photons $3 < E_T^\gamma < 10$ GeV and for the pseudorapidity range of the photons $-1.2 < \eta^\gamma < 1.8$. They are measured differentially as a function of E_T^γ and η^γ. The results are compared with the predictions of a new leading order calculation, which is in reasonable agreement with the inclusive measurement. Comparisons with the predictions of the event generators PYTHIA and HERWIG are also presented.

1 Introduction

Isolated photons with high transverse momentum in the final state are a direct probe of the dynamics of the hard subprocess, since they are directly observable without large corrections due to hadronisation and fragmentation. Previously ZEUS and H1 have measured the prompt photon cross section in photoproduction[1][2]. ZEUS has recently published an analysis of the prompt photon cross section for photon virtualities Q^2 larger than 35 GeV^2[3]. The results are compared to a new leading order calculation[4][5], $\mathcal{O}(\alpha^3)$, that offers first predictions for the inclusive prompt photon production in Deep Inelastic Scattering.

2 Experimental Technique

The events have been collected with the H1 detector([6]) at HERA in the years 99/00 at a center of mass energy of 318 GeV, with a total integrated luminosity of 70.6 pb^{-1}.

Events were selected with the electron reconstucted in the backward calorimeter (SpaCal[7]). Photons are identified in the H1 liquid argon calorimeter (LAR)[8] by a compact electromagnetic cluster with no track pointing to it. The transverse energy is restricted to 3 GeV$< E_t^\gamma <$ 10 GeV in the pseudorapidity region $-1.2 < \eta_\gamma < 1.8$[1] The main experimental difficulty is the separation of the photons from neutral mesons, mainly π^0 or η, since at high energies their decay photons are not resolved but reconstructed in one single electromagnetic cluster. These mesons are mainly produced in hadronic jets, therefore an isolation criterium is applied for the γ candidates. To ease the comparison with pQCD calculations we use an infrared-safe definition of the isolation requirement[9][10]: the energy fraction z of the photon energy to the energy of the jet which contains the photon (Photonjet) has to be larger than 0.9.

$$z = E^\gamma / E^{Photonjet} > 0.9 \tag{1}$$

After the selection cuts there is still a large fraction of background from neutral mesons. The photon signal is extracted by a shower shape analysis which uses six discriminating shower shape functions in a likelihood analysis.
The data are corrected for detector effects by taking the average of the corrections of the PYTHIA 6.2[11] and the HERWIG 6.5[12] event generator. The background from neutral mesons was generated with the RAPGAP[13] generator. However, the background Monte Carlo was only used to control the sample not for the extraction of the signal. This was done using single particles only.

3 Event Selection

The main experimental requirements for the selection of the events are the following:

[1]The pseudorapidity η of a particle with polar angle θ is given by $\eta = -\ln\tan(\theta/2)$. θ is measured with respect to the z-axis with the positive axis defined by the direction of the proton, hence positive η points in the direction of the proton.

- Events are triggered by an electromagnetic cluster in the SpaCal. The trigger efficiency is close to 100%.
- Electron Selection: well identified electron reconstructed in the backward calorimeter ($151^\circ < \theta_e < 177^\circ$) with an energy larger than 10 GeV.
- $Q_e^2 > 4$ GeV^2, inelasticity $y_e = 1 - E'_e(1 - \cos\theta_e)/2E_e > 0.05$, where E'_e is the energy of the scattered electron.
- 35 GeV$< \Sigma(E - p_z) < 70$ GeV, where the sum runs over all the particles and p_z is their longitudinal momentum. This cut suppresses photoproduction background.
- Vertex: the event vertex is required to be within 40 cm of the nominal vertex position. There has to be at least one good reconstructed track apart from the track pointing to the electron. This ensures a good vertex reconstruction and suppresses background from elastic QED compton events.
- Jets: at least one jet with transverse momentum larger than 2.5 GeV and $\eta_{jet} < 2.1$. The jet is reconstructed using the k_t algorithm with cone size $R_0 = 1$[14]. If only one jet is found, the jet is bound to be the Photonjet.
- Photon candidate: electromagnetic cluster with $3 < E_T^\gamma < 10$ GeV and pseudorapidity $-1.2 < \eta^\gamma < 1.8$. No track is allowed to point to the photon candidate within 20 cm. The cluster has to be compact with a transverse radius of less than 6 cm. The invariant mass of the cluster combined with the closest electromagnetic neighbour with an energy above 80 MeV must be larger than 0.3 GeV. This requirement rejects candidates from π^0 decays with the two photons reconstruced in individual clusters. Candidates close to the cracks of the calorimeter are rejected.
- Isolation: the energy fraction of the photon energy to the energy of the photon jet z has to be larger than 0.9.

In a first step events are selected with a good electron and a jet which contains a photon candidate as defined above. In a second step the prompt photon signal is extracted by a likelihood analysis of the shower shapes.

4 Extraction of the prompt photon signal

The photon candidate clusters are analysed using six different shower shape variables to discriminate between the signal of a single photon and neutral mesons.

- Hot core fraction: fraction of energy deposited in four or eight - depending on the granularity of the calorimeter - contiguous cells including the cell with highest energy.
- Transverse radius of the cluster (transverse plane is perpendicular to the direction of the incoming particle).

- Energy fraction of the hottest cell.
- Energy fraction in the first layer.
- Kurtosis of the transverse energy distribution of the cluster cells.
- Transverse Symmetry of the cluster: a photon is expected to have a symmetric cluster (S=1), whereas neutral mesons with more than one decay photon are of more asymmetric shape.

Figure 1 shows the six different shower shape variables together with the background from RAPGAP as well as photons radiated off the electron as predicted by RAPGAP and the signal prediction from PYTHIA (scaled by 2.3) for photons being radiated off the quark. Both contributions from RAPGAP are used unscaled. All variables are nicely described by the sum of the Monte Carlo predictions. The estimators are combined in a likelihood analysis as well as

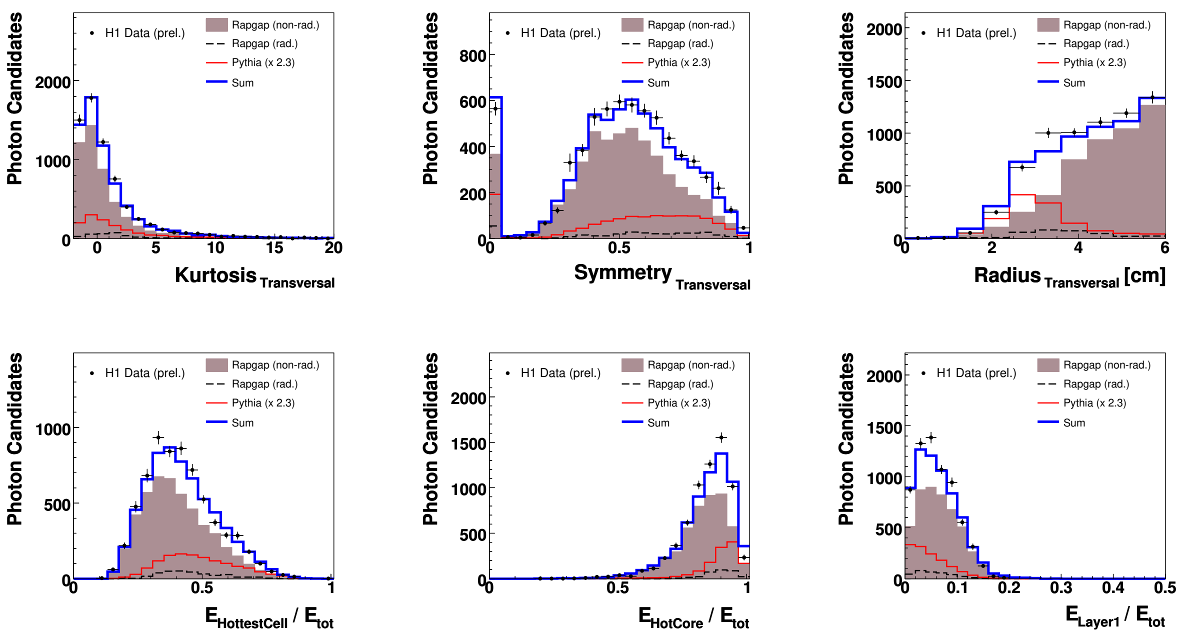

Figure 1: Shower shape variables used as input for the discrimination between the photon and neutral mesons: Transverse kurtosis, symmetry and radius and energy fractions of the hottest cell, the hot core and the first layer). The measured data points are shown together with the signal Monte Carlo from PYTHIA, scaled by a factor 2.3, photons radiated off the incoming or outgoing electron (rad) and background from neutral mesons (non-rad) as estimated by RAPGAP. The contributions from RAPGAP are used unscaled. The sum of the Monte Carlo prediction is indicated by the blue line.

a neural net and a range search analysis as a cross check. Monte Carlo studies showed that neutral mesons can be well separated from photons for transverse energies below 10 GeV. Only particles which decay very asymmetrically are misidentified as photons.

The likelihood distribution which has a good separation power is shown in Figure 2 together with the background from RAPGAP and the signal from PYTHIA plus radiative photons from RAPGAP. The data is well described by the sum of the predictions. Also the fraction of neutral mesons is well predicted by the unscaled RAPGAP background, which accumulates at low likelihood values.
The probability densities that are used for the likelihood method are taken from the simulation of single particles. Only the contributing fraction of any neutral meson (π^0, η^0, η', K^0, ρ, ω, $K^\star$, K_L,K_s, n and $\bar{n}$) is taken from Monte Carlo simulation (RAPGAP). The likelihood functions are calculated separately for different bins in E_T and different wheels of the calorimeter[8] which correspond to different η_γ ranges. The contribution of photons and neutral mesons is then determined by independent fits to the data using likelihood distributions obtained from a set of single particle photons and background respectively. The advantage of the use of single particles is that they can easily be produced in high statistics.

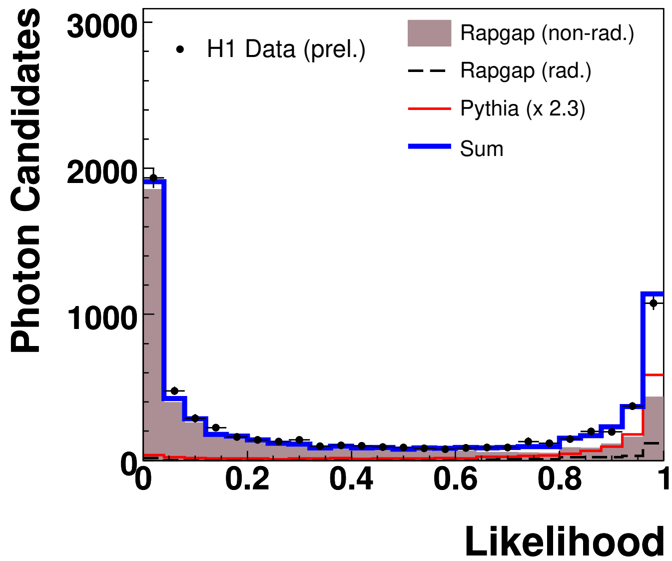

Figure 2: Likelihood Distribution of photon candidates that have passed the primal event selection.

5 Systematic errors

Various systematic uncertainties were considered. The total systematic error per bin is obtained by adding all different systematic errors in quadrature. The dominant errors are

- Photon energy: the energy scale at the energies used in this analysis was checked with the reconstructed π^0 mass and found to be well calibrated. An error of $1\% - 3\%$ (forward region) was assumed. This results in a systematic error of the cross section of at most 12%.

- Electron energy: an uncertainty of 2%is applied to the energy of the scattered electron.
- An important error is the description of the shower shape variables in the simulation. The differences between simulation and data were studied using electrons in NC DIS events, systematic errors between 3.5% and 8% were applied.
- Model dependence: the model dependence was studied by comparing HERWIG and PYTHIA, in the forward region it leads to an error of up to 22%.

6 Results

Differential cross sections for the production of isolated photons in deep inelastic scattering are shown for $Q_e^2 > 4$ GeV^2, $y_e > 0.05$ for photons with $3 < E_T^\gamma < 10$ GeV, pseudorapidity $-1.2 < \eta^\gamma < 1.8$ and the isolation $z = E_\gamma / E_{\gamma Jet} > 0.9$. The errors in the figures contain the statistical error and the systematic errors added in quadrature.

Figure 3 shows the cross section as a function of transverse energy and the pseudorapidity compared to the prediction of the PYTHIA and HERWIG generator (radiation off the quark) plus photon radiation off the electron. Both generators nicely describe the shape in E_T but are significantly lower in the abolute scale (factor 2.3 for PYTHIA and 2.6 for HERWIG in order to match the total cross section). The η distribution is described somewhat better by PYTHIA. At low η the production of isolated photons is dominated by radiation off the electrons, which becomes negligible at pseudorapidities larger than 0.

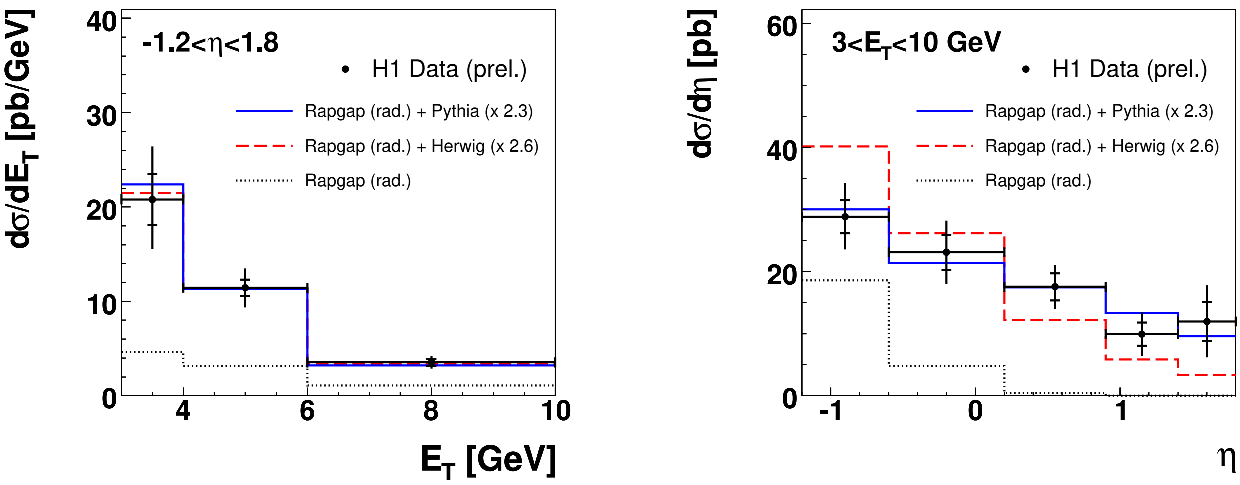

Figure 3: Prompt photon differential cross sections $d\sigma/dE_T^\gamma$ for $-1.2 < \eta^\gamma < 1.8$ (a) and $d\sigma/dE_\eta^\gamma$ for $3 < E_T^\gamma < 10$ GeV (b), for photon virtualities $Q^2 > 4$ GeV^2 and $y_e > 0.05$. The measured cross section is compared to the prediction of PYTHIA (scaled 2.3) and HERWIG (scaled 2.6) plus radiation off the electron, Rapgap(rad).

Figure 4 shows the comparison with a new LO (α^3) calculation[4][5] which gives a good description of the data. At large pseudorapidities the dominant contribution comes from radiation off the quark line (QQ), whereas in the backward region the radiation off the electron line (LL) dominates the cross section. The data is slightly higher than the calculation. Figure 5 shows the differential cross section $d\sigma/dE_T^\gamma$ in five different η-regions which correspond to individual wheels of the calorimeter. In all five η regions the data is well described by the LO (α^3) calculation.

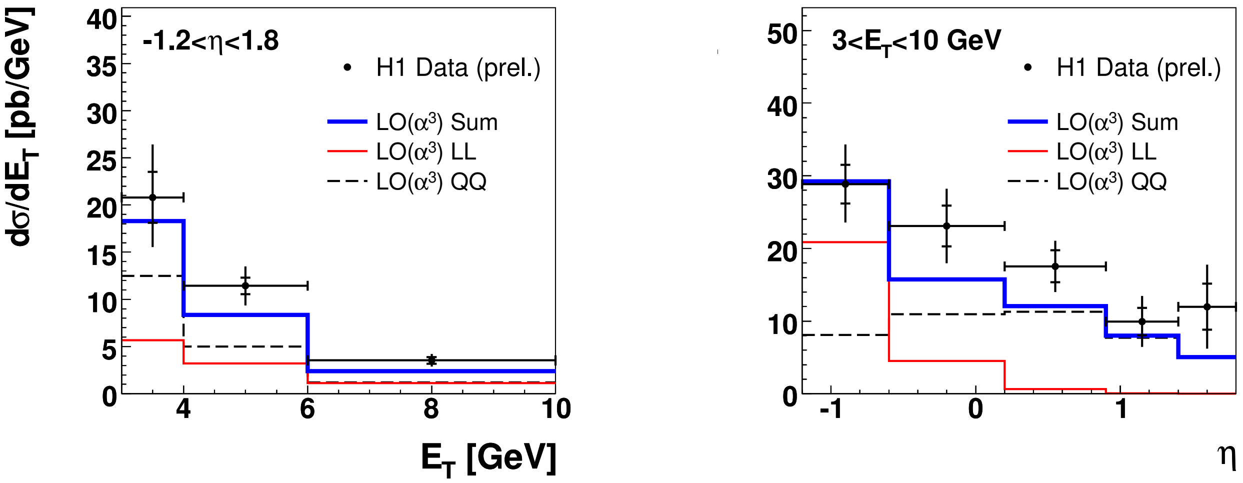

Figure 4: Prompt photon differential cross sections $d\sigma/dE_T^\gamma$ for $-1.2 < \eta^\gamma < 1.8$ (a) and $d\sigma/d\eta^\gamma$ (b) for $3 < E_T^\gamma < 10$ GeV, for photon virtualities Q^2 >4 GeV^2 and $y_e > 0.05$ compared to a LO calculation[4][5]. LL and QQ show the contribution of radiation off the electron and the quark line respectively. As the interference is very small it is not shown, but included in the sum.

7 Conclusion

Results on inclusive prompt photon production in deep inelastic scattering have been presented. The data is nicely described in shape by PYTHIA generator plus radiation off the electron line as modelled by RAPGAP, though the absolute scale is too low. The HERWIG generator together with radiative photons shows a somewhat stronger η dependence than the data and is also too low in scale. The data is reasonably described in the covered η^γ and E$_T^\gamma$ range by a new perturbative LO (α^3) calculation.

Acknowledgements
We'd like to thank Aude Gehrmann-de Ridder, Thomas Gehrmann and Eva Poulsen for providing the LO calculations and many fruitful discussions.

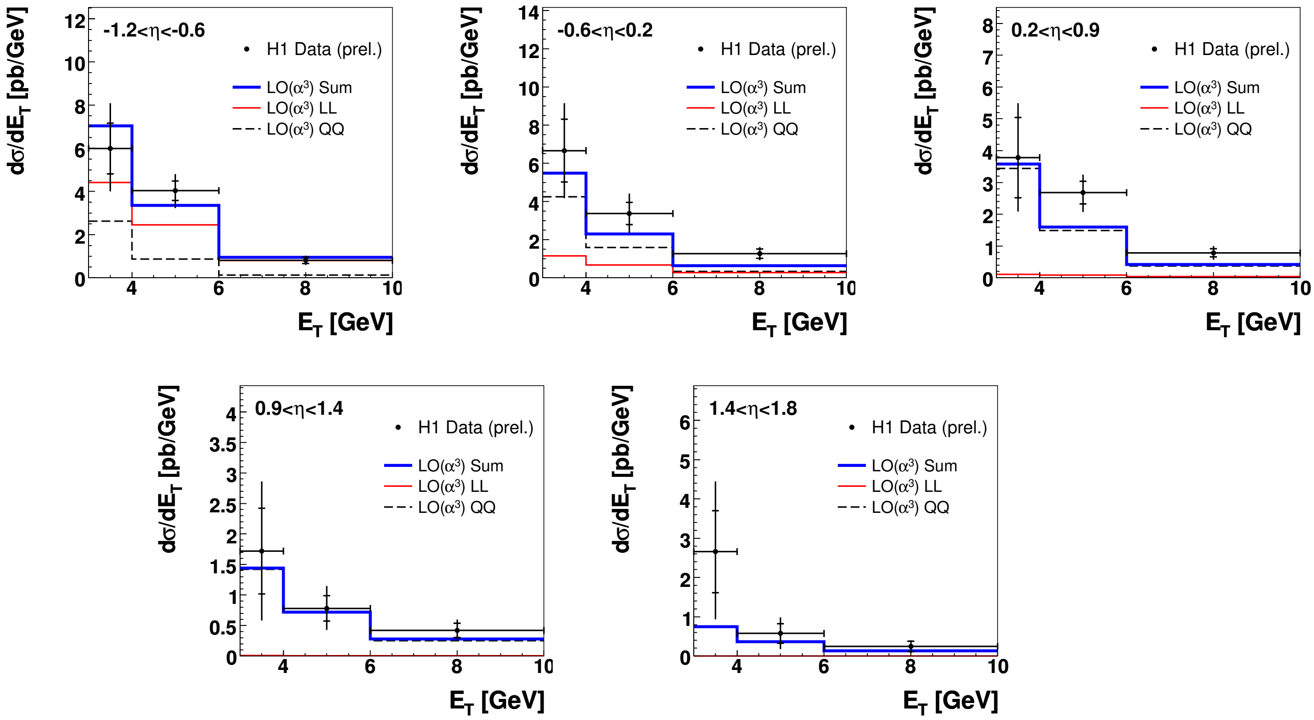

Figure 5: Prompt photon differential cross sections $d\sigma/dE_T^\gamma$ in five different bins in η for photon virtualities Q^2 >4 GeV^2 and $y_e > 0.05$ compared to a LO calculation[4][5].

References

[1] J. Breitweg *et al.* [ZEUS Collaboration], Phys. Lett.**B 472** (2000) 175 [hep-ex/9910045].

[2] A. Aktas *et al.* [H1 Collaboration], Eur. Phys. J.**C38** (2005) 437 [hep-ex/0407018].

[3] S. Chekanov *et al.* [ZEUS Collaboration], Phys. Lett.**B 595** (2004) 86 [hep-ex/0402019].

[4] A. Gehrmann-De Ridder, T. Gehrmann and E. Poulsen, Phys/ Rev.. Lett. (in press) [hep-ph/0601073].

[5] A. Gehrmann-De Ridder, T. Gehrmann and E. Poulsen [hep-ph/0604030].

[6] I. Abt *et al.* [H1 Collaboration] Nucl. Instr. and Meth. **A 386** (1997) 310, ibid, 348.

[7] T. Nicholls *et al.* [H1 SPACAL Group], Nucl. Instrum. Meth. A **374** (1996) 149.

[8] B. Andrieu *et al.* [H1 Calorimeter Group Collaboration], Nuc l. Instrum. Meth. A**336** (1993) 460.

[9] E. W. N. Glover and A. G. Morgan, Z. Phys. C **62** (1994) 311.

[10] D. Buskulic *et al.* [ALEPH Collaboration], Z. Phys. C **69** (1996) 365.

[11] T. Sjöstrand *et al.*, PYTHIA 6.2 Physics and Manual [hep-ph/0108264].

[12] G. Corcella *et al.*, HERWIG 6.5 Release Note **135** (2001) 128 [hep-ph/0210213].

[13] H. Jung, Comput. Phys. Commun. **86** (1995) 147
(see also http://www.desy.de/ jung/rapgap.html).

[14] Stephen D. Ellis, Davison E. Soper, Phys.Rev. **D48** (1993) 3160 [hep-ph/9305266].